Reviews on Advanced Materials and Technologies, 2025, vol. 7, no. 2, pp. 88–104
DOI: 10.17586/2687-0568-2025-7-2-88-104

# Progress and Perspectives of Physics-Informed Neural Networks for Tribological Applications with Multiphysics Awareness

**A.Yu. Kokhanovskiy [1], L.M. Dorogin [2,3], X.A. Egorova [4], E.V. Antonov [2,*], D.A. Sinev [4]**

[1] Faculty of Physics , ITMO University, Kronverkskiy pr., 49, lit. A, St. Petersburg, 197101, Russia
[2] Institute of Advanced Data Transfer Systems, ITMO University, Kronverkskiy pr., 49, lit. A, St. Petersburg, 197101, Russia
[3] Department of Molecules and Materials, University of Twente, Enschede, The Netherlands
[4] Institute of Laser Technologies, ITMO University, Kronverkskiy pr., 49, lit. A, St. Petersburg, 197101, Russia

**Article history**

Received April 08, 2025
Received in revised form, May 14, 2025
Accepted May 16, 2025
Available online May 26, 2025

**Abstract**

Recent advancements in the field of physics-informed neural networks (PINNs) hold great potential for solving the tribology-related problems, and areas for their applications are systematically reviewed in this article. The tribological applications are viewed as fundamentally dependent on the variety of multiphysics phenomena, which must be taken into account when developing PINNs. Materials data, topology and surface roughness, and analytical tribometry data can be used as multiphysics input for the PINNs specialized in solving friction, lubrication, wear, wetting, heat transfer, structural and phase transitions, chemical reactions, cracking, and fretting problems. Creating multi-PINNs that synthesize the individual tribology phenomena into the complex multiagent approach is viewed as a practically important and challenging issue that is yet to be addressed.

Keywords: Tribology; Friction; Neural network; Multiphysics; Machine learning

## 1. INTRODUCTION

Tribology is one of the most important and at the same time very complex part of materials science [1,2]. Natural phenomena (such as earthquakes), biological systems (such as joints), mechanical and anthropogenic devices—all are based on processes that take place in various types of contact (tribological) systems. The problem of creating materials with specified tribological properties is directly linked to important applications in various industries but is still far from being solved. High friction can lead to wear and reduction of products service life in mechanical engineering, which has great economic and environmental impact. It was estimated that more than half of the fuel consumed by cars and other vehicles is wasted on overcoming friction in moving joints.

The problem of friction control is very complex from a scientific point of view due to the variety of physics phenomena accompanying friction processes, which may include the presence of contaminants, the presence of liquids and capillary phenomena, surface defects, etc. Tribology as a scientific discipline is difficult to generalize. This is due, in particular, to the fact that the state of real surfaces during contact is difficult to determine due to surface roughness and contamination, which greatly affect contact phenomena [3]. Even a theoretically formally defined surface contains an incredible number of degrees of freedom, which can hardly be calculated by direct methods [4]. Therefore, numerous phenomenological models of contact mechanics, in particular, friction models, usually choose one predominant friction mechanism and neglect others. Knowledge about small tribological systems and friction on the nanoscale, forming the discipline of nanotribology, can be also helpful in understanding tribology at the macroscale [5,6].

All tribological phenomena are governed by atomistic interaction inside the contacting solids, between them, and in the liquid or solid substances present at the interface. Those interactions manifest themselves via various physical phenomena, that can be described by respective

* Corresponding author: E.V. Antonov, e-mail: evantonov@itmo.ru

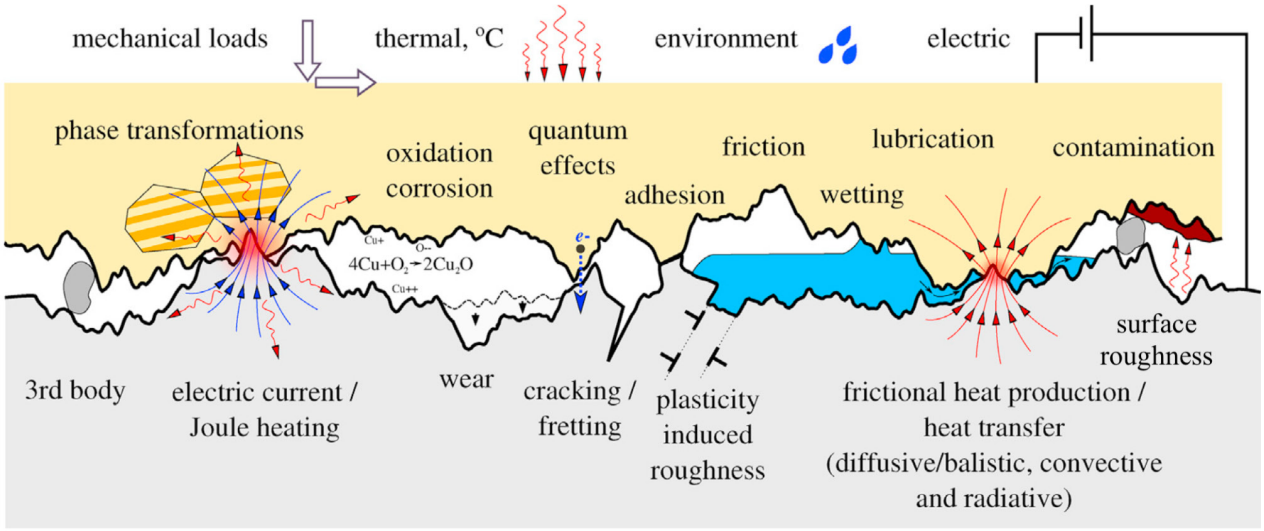


**Fig. 1.** Scheme representing a variety of physical phenomena in a tribological system illustrated by two different solid materials with surface roughness brought into mechanical contact. The tribological system is exposed to various loads: mechanical, thermal, electric, and environmental. Adapted from Ref. [3].

theories and models. Thus, the tribological interface can be viewed as multiphysics system, containing multiple coupled fields (see Fig. 1), involving mechanical, thermodynamic, electro-magnetic, chemical, quantum, and other types of phenomena [3].

Analytical models in tribology commonly make use of simplifications that exclude certain physical phenomena, and, thus, are prone to inaccuracies. Tribological experiments can be expensive and time-consuming. Physics-informed machine learning is a technique that can improve traditional models, increase their accuracy and robustness for applications in friction, wear prediction and lubrication by integrating data with mathematically formulated physics models [7–9]. Combining the classical data-driven approach with physics equations into neural networks, so-called physics-informed neural networks (PINNs) can be realized. The underlying equations of physics laws can be incorporated in PINN through residual terms. PINN is meshless—one of the main advantages of using PINNs over finite element method (FEM). In the following sections of the paper, recent progress in PINNs development in several most common tribology-related fields, including lubrication, friction, wear, heat transfer, chemical reactions, wetting, phase transitions, cracking, and fretting is considered.

## 2. SPECIALIZED TRIBOLOGY-ASSOCIATED PINNs

### 2.1. Lubrication

Lubrication critically enhances the reliability and durability of mechanical systems by minimizing friction, wear, and thermal degradation at contact surfaces. Effective lubrication reduces direct metal-to-metal contact, dissipates heat generated during operation, and prevents material loss or deformation. By maintaining optimal interfacial conditions and preventing corrosion or adhesive failure, lubrication directly governs the operational longevity and maintenance intervals of mechanical systems [10]. In lubricated tribological contact elastohydrodynamic lubrication (EHL) numerical simulations commonly rely on the Reynolds equation to compute contact surface deformation and pressure distribution. In the recent publication [11], the potential capability of PINNs in addressing EHL via Reynolds equation under conditions of sliding and squeezing in contact (Fig. 2), and transient cavitation had been revealed. In the lubrication problems for finding the pressure distribution of thin viscous fluid films PINNs commonly include the loss function as shown in Fig. 2.
In the paper [12] a hybrid method for prediction of lubrication phenomena with classical graph neural networks as well as PINNs was employed, which allowed to demonstrate improved accuracy with the described method. The decision tree algorithm was used for classification problem that defines the lubrication success or lubrication failure. The neural network can predict the lubrication thickness as feeding input to the physics-informed network, which in its turn can predict pressure and thickness distribution of the lubricant film.

Rom [13] demonstrated on the example of a journal bearing, that the PINN solves several problems simultaneously and generalizes the replicable solution by extending its inputs such as the relative eccentricity of a bearing. Accurate pressure and liquid ratio predictions for further values of the relative eccentricity are then obtained by just evaluating the PINN taking less than a second. The model allows to consider cavitation phenomena by modifying

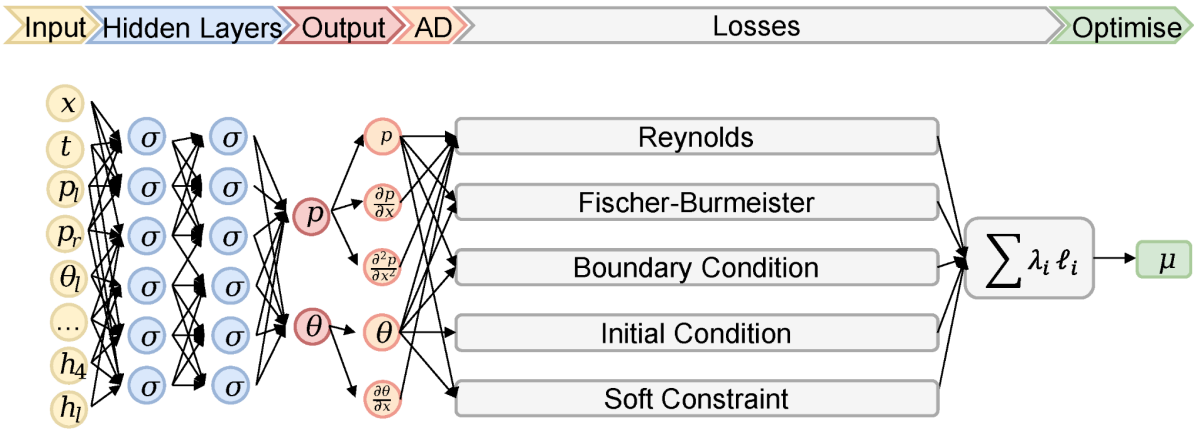


**Fig. 2.** Schematic illustration of a hydrodynamic lubrication PINN framework. Reprinted from Ref. [11], © 2024 by Faras Brumand-Poor et al. Available under the terms of the CC BY 4.0 license.

the Reynolds equation by introducing the liquid fraction function $\theta(x, y)$. Results have confirmed that the deviations of the PINN solutions from the reference solutions are quite small (0.6%, 0.7% and 1.6%). Furthermore, a maximum relative error of 1.6% is clearly acceptable given the computation time is reduced to less than a second when evaluating the trained neural network.

In the paper [14] PINN was applied to solve an initial value problem described by a first order ordinary differential equation (ODE) and to solve the Reynolds boundary value problem, described by a second order ODE. Both these problems were selected since they can be solved analytically, and the error analysis showed that the predictions returned by the PINN were in good agreement with the analytical solutions for the given specifications.

In the paper by Zhou et al. [15] an alternative approach to PINN model by augmented Lagrangian method (ALM) is demonstrated. This approach includes incorporating penalty terms and simulating Lagrange multipliers and redefining the boundary value problem as an unconstrained optimization problem, solved by minimizing the Lagrangian function. ALM adaptively adjusts the weights of each constraint according to each collocation point error, thereby steering the solution toward accuracy. ALM-PINNs loss function can be formulated as follows:

$$l_{\lambda}^{k} = \omega_f l_f + \omega_b l_b + \frac{1}{M}\sum_{j=1}^{M} \lambda_j^k \left(\bar{x}_j \bar{y}_j\right) b\left(\bar{x}_j \bar{y}_j \boldsymbol{\omega}^k\right), \quad (1)$$

where $\omega_f$ and $\omega_b$ represent the fixed penalty coefficients of the partial differential equation (PDE) residuals $f$ and boundary errors $b$ in the loss function, respectively, $l_f$ is the residuals of the Reynolds equation and $l_b$ is the errors of boundary conditions, $M$ is the number of collocation points on the boundary located at the dimensionless coordinates $\bar{x}_j$ and $\bar{y}_j$, the third term on the right of the equation is the Lagrangian term, and $\lambda_j^k$ represents the Lagrange multiplier, $\boldsymbol{\omega}^k$ is the weight of the $k$-th hidden layer. ALM-PINNs significantly improved boundary accuracy compared to other types of PINNs, adaptively balancing the weights of loss during training. The maximum boundary error was reduced by approximately 80%.

### 2.2. Friction

Friction critically influences the reliability and durability of mechanical systems by governing wear rates, heat generation, and energy dissipation at contact interfaces. Excessive friction accelerates material degradation through adhesive, abrasive, or fatigue mechanisms, particularly in components like bearings and mining machinery operating in aggressive environments [16]. However, controlled friction remains essential for functionality in systems such as clutches or braking mechanisms, and is necessary to predict, control, and apply. The paper by Olejnik et al. [17] revisits the static and dynamic friction models, including Coulomb, Coulomb-viscous, Stribeck, Dahl, LuGre and generalized Maxwell-slip models and demonstrates application of PINNs to the problem planar friction of a double torsion pendulum system. It was shown that the model computational effort is moderate and it exhibited high accuracy in predicting the angular rotation of the disk pendulum (Fig. 3).

In the study [18] a PINN model incorporating basic heat transfer PDE and various types of boundary conditions into neural networks, is proposed to solve forward and inverse problems of frictional contact temperature. The loss function was derived from the equation of thermal conductivity with boundary conditions, supported by experimental or FEM-generated data (Fig. 4).

The inverse problem was defined as restoring of heat partitioning coefficient (HPC) and convective heat transfer coefficient (CHTC) from a limited set of temperature data. The authors stated that the PINN demonstrates the capability to predict accurately the frictional contact tem-

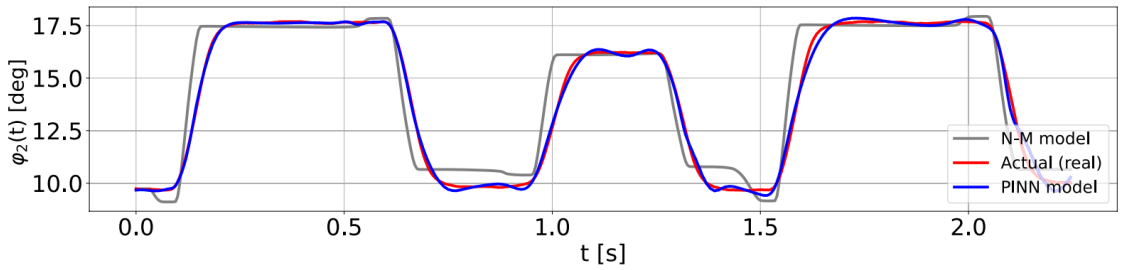


(a) disk pendulum angular position

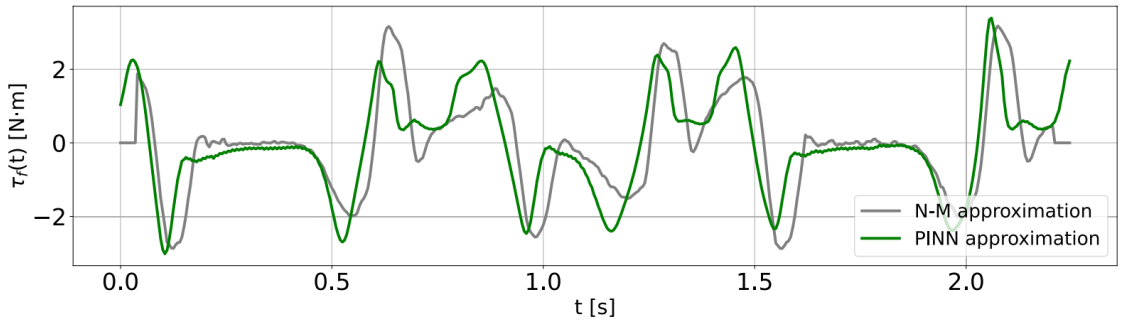


(b) friction torque

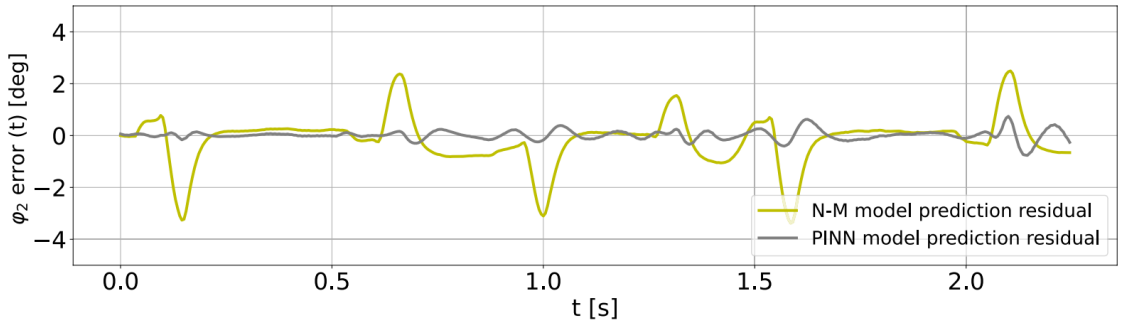


(c) error of the model prediction

**Fig. 3.** Results of prediction of the frictional torque characteristics with the use of two identification models: PINN and model by Nelder-Mead algorithm (N-M). Reprinted from Ref. [17], © 2023 P. Olejnik and S. Ayankoso. Available under the terms of the CC BY 4.0 license.

perature field by incorporating just a single actual temperature data point during training. When an input thermal parameter, such as HPC or CHTC, is unknown, the PINN demonstrates the capability to accurately predict the frictional contact temperature field by incorporating just a single actual temperature data point during training, with a mean relative error (MRE) of about 0.01–0.001%, and simultaneously, HPC and CHTC can be precisely identified by the optimization process of the PINN, with the relative error of about 0.01–0.1%. Experimental analysis revealed that the sampling positions of actual data play a significant role in influencing the predictive performance of the PINN. Incorporating actual data, which are strongly influenced by boundary conditions, into the training process can enhance the effectiveness of the PINN for solving inverse problems. Finally, the study investigated the inverse thermal problem with multiple unknown input thermal parameters. The experimental results indicate that the PINN is successful at resolving cases involving two unknown CHTCs; the relative error of CHTCs is about 1–3%. Incorporating a limited actual temperature data into the PINN can substantially enhance the accuracy of the frictional contact temperature field when all input thermal parameters are unknown, and the MRE of the temperature field decreases from 5.16% to 0.79%.

### 2.3. Wear

Physics-informed machine learning has become a powerful approach to improve the prediction accuracy of wear

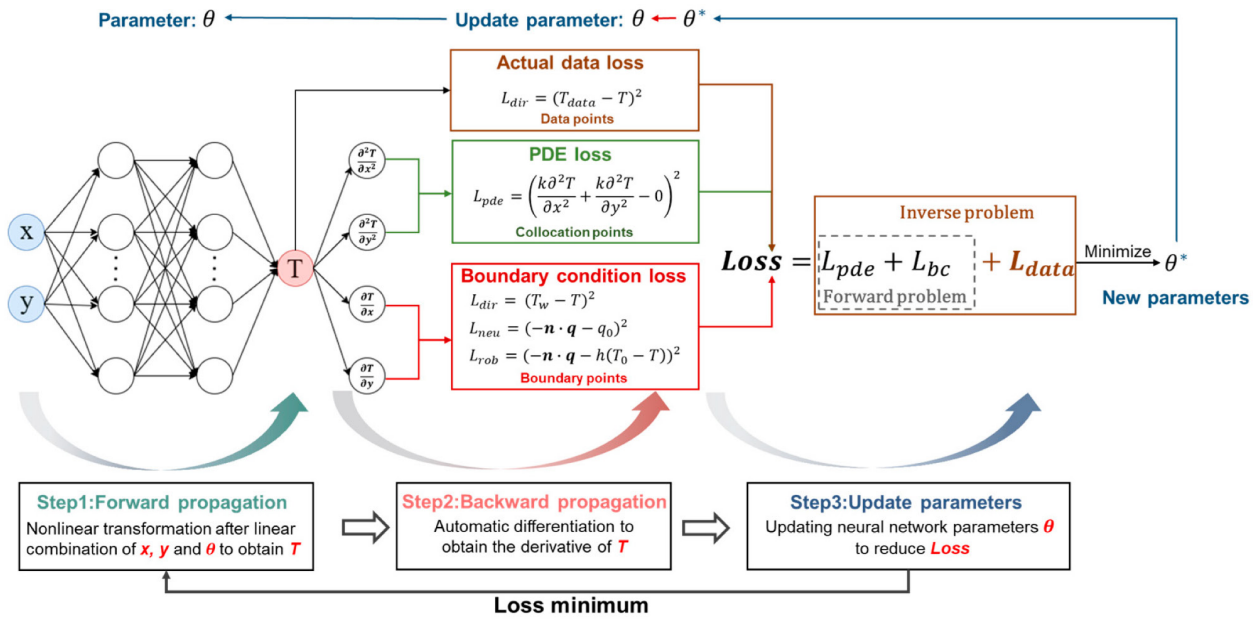


**Fig. 4.** Simulation of frictional contact temperature based on the PINN. Reprinted from Ref. [18], © 2024 by Y. Xia and Y. Meng. Available under the terms of the CC BY 4.0 license.

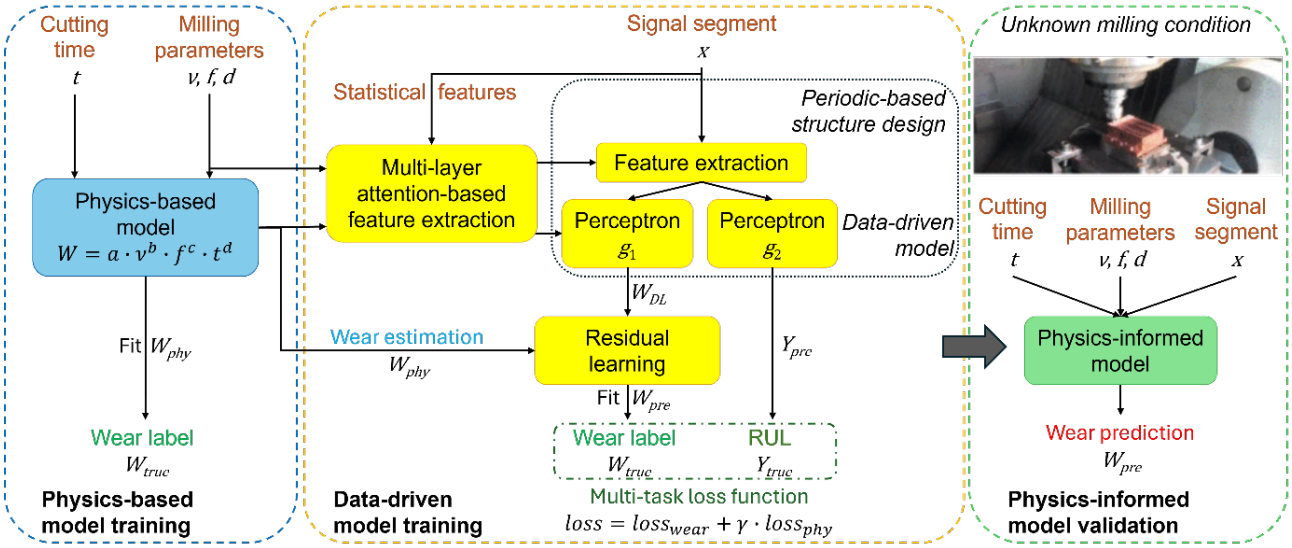


**Fig. 5.** The tool wear monitoring framework based on physics-informed machine learning (RUL means remaining useful life). This figure is a sketch of Fig. 1 from Ref. [20]; all major designations are saved.

rates in manufacturing processes by integrating physical laws with data-driven models. Jakubowski et al. [19] have used a physics-informed autoencoder in a semi-supervised manner to learn the degradation process of work rolls in the cold-rolling process and have shown that such an architecture is capable of distinguishing between low- and high-wear observations. Later, Zhu et al. [20] considered the use of PINN in the problem of high-speed milling using bidirectional long short-term memory network (LSTM) and fully connected neural networks (Fig. 5). The phenomenological models of partial wear extended Taylor's equation were used as physical models [21]. Ultimately, the model predicted tool wear depending on the operating time. The authors compared the performance of different algorithms and found that the attention-based dual-scale hierarchical LSTM model in combination with a PINN and the extended Taylor's equation model provided the most accurate results, decreasing prediction errors by 42%.

### 2.4. Heat and mass transfer

Heat transfer plays a crucial role in determining the reliability and durability of mechanical systems subject to abrasive wear. Efficient heat dissipation is essential for maintaining optimal operating temperatures, which helps

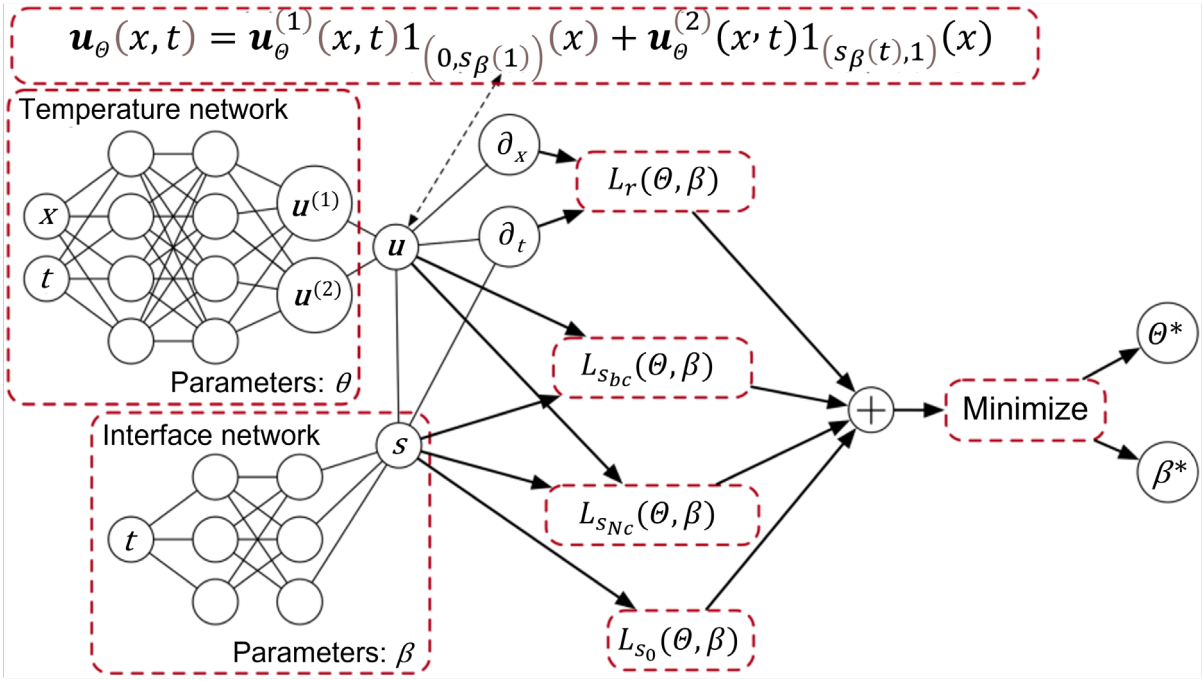


**Fig. 6.** Two-phase Stefan problem: PINN architecture for inferring the latent temperature fields $u_1(x,t)$ and $u_2(x,t)$, and phase-transition interface $s(t)$, from scattered noisy observations of temperature. Adapted from Ref. [25].

prevent overheating that can lead to material degradation and mechanical failure. In systems like automotive brake discs, heat transfer is vital for dissipating the thermal energy generated during braking, ensuring consistent performance and longevity [22]. Similarly, in electronic devices, advanced cooling techniques such as microchannel and pin-fin structures enhance heat transfer, reducing thermal stress and improving device reliability [23]. Poor heat management can lead to increased wear and reduced lifespan of components, highlighting the importance of modeling the effective thermal management.

PINNs have shown great potential to predict temperature and velocity fields for the heat management tasks without relying on extensive simulation data or mesh generation [24]. PINNs have been applied to various scenarios, including forced and mixed convection with unknown thermal boundary conditions, and the Stefan problem for two-phase flow [25]. Solutions of this problem are based on the incompressible Navier–Stokes equations and the corresponding temperature equation:

$$\frac{\partial\Theta}{\partial t}+(\boldsymbol{u}\cdot\nabla)\Theta=\frac{1}{N_{\mathrm{Pe}}}\nabla^2\Theta,$$

$$\frac{\partial\boldsymbol{u}}{\partial t}+(\boldsymbol{u}\cdot\nabla)\boldsymbol{u}=-\nabla p+\frac{1}{N_{\mathrm{Re}}}\nabla^2\boldsymbol{u}+N_{\mathrm{Ri}}\,\Theta,$$

$$\nabla\cdot\boldsymbol{u}=0, \tag{2}$$

where $\Theta$, $\boldsymbol{u}=(u,v)^T$, and $p$ are the dimensionless temperature, velocity, and pressure fields, respectively. $N_{\mathrm{Pe}}$, $N_{\mathrm{Re}}$, and $N_{\mathrm{Ri}}$ denote the Peclet, Reynolds, and Richardson numbers, respectively. To consider heat transfer in a two-phase system, equations were set for the latent temperature distributions within each of the two phases, $u_1(x,t)$ and $u_2(x,t)$, respectively, that satisfy a heat equation

$$\frac{\partial u_a}{\partial t}=k_a\frac{\partial^2 u_a}{\partial x^2},\quad (x,t)\in\Omega_a,\quad a=1,2, \tag{3}$$

where $k_1$, $k_2$ are thermal diffusivity parameters. PINN structure for solving the two-phase Stefan problem is shown in the Fig. 6. Inspired by PINN, an auto encoder and image gradient-based approach has also been proposed by the Central ML Team at Ansys team for solving 2D and 3D chip thermal analysis [26]. The proposed network shows acceptable agreement with numerical simulation with mean absolute percentage error of 0.4%.

Furthermore, Laubscher et al. [27] have shown the applicability of PINN modeling methodologies to solve simple multi-species flow and heat transfer on a 2D rectangular domain. To solve the laminar steady-state transport of mass, momentum, species, and energy throughout the domain requires the simultaneous solution of the following PDEs:

- mass transport

$$\nabla\cdot\boldsymbol{u}=0, \tag{4}$$

where $\boldsymbol{u}=(u,v)$, $u$ and $v$ are the inlet $X$- and $Y$-velocities, respectively;

- momentum transport

$$\rho\nabla\cdot(\boldsymbol{uu})=\mu\nabla\cdot(\nabla u)-\nabla p, \tag{5}$$

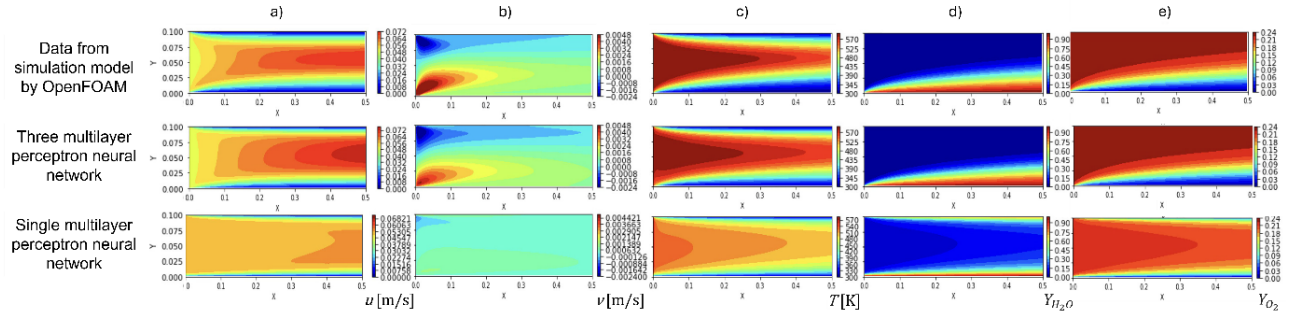


**Fig. 7.** Velocity (a, b), temperature (c) and species mass fraction (d, e) predictions. Adapted from Ref. [27].

where ρ is the density, μ is the viscosity of the fluid mixture and $p$ is the outlet pressure;

- species transport

$$\rho\nabla\cdot\left(\boldsymbol{u}Y_i\right)=\rho D_m\nabla\cdot\left(\nabla Y_i\right)-\nabla p, \tag{6}$$

where $Y_i$ is the species mass fraction of the gas component $i = O_2$, $N_2$, $H_2O$ and $D_m$ is the mixture molecular diffusion coefficient;

- energy transport

$$\rho\nabla\cdot\left(\boldsymbol{u}c_{P,m}T\right)=\nabla\cdot\left(\lambda\nabla T\right)-\rho D_m\nabla\cdot\left(\sum_{i=1}^{3}h_i\nabla Y_i\right), \tag{7}$$

where $c_{P,m}$ is specific heat capacity of the gas mixture, $T$ is the temperature and λ is the thermal conductivity coefficient, $h_i$ is the enthalpy of the corresponding species. Two PINN models (PINN-1 and PINN-3) were developed and compared in the test conditions of simulating the propagation of water vapor into dry air flowing in a duct. PINN-1 used a single network to predict the mass, momentum, species, and energy equation quantities, whereas PINN-3 used a PINN for each set of physics PDEs being solved (one for mass and momentum PDEs, one for all the species PDEs, and one for the energy PDEs). The results of two PINN models were compared to simulation data taken from a traditional computational fluid dynamic simulation model prepared in an open-source fluid flow simulation library OpenFOAM (Fig. 7). The results showed that for nearly all cases the PINN-3 approach yielded lower loss values compared to the resultant PINN-1 losses. On average, for all the models trained, the PINN-3 losses were 62% lower compared the PINN-1 values. The results showed that the single network approach could adequately resolve the momentum and energy PDEs, but struggled to enforce the species mass transport requirements, whereas the PINN-3 approach successfully resolved the physics PDEs.

PINNs have also been used to solve inverse heat transfer problems, estimating unknown material properties and boundary conditions from limited experimental data [28]. PINNs have demonstrated robustness in handling noisy data and partially missing physics, making them suitable for realistic industrial applications [25,28]. Furthermore, physics-informed activation functions enable accurate predictions beyond the training zone, outperforming theory-agnostic machine learning methods in heat transfer applications [29]. Interestingly enough, PINN applications for heat and mass transfer analysis might be further expanded into the chemistry domain [30], including reaction kinetics modeling (e.g., predictions of reaction networks, kinetic parameters, and species production) and reaction condition optimization (see the next Section).

### 2.5. Chemical reactions

Chemical reactions can lead to corrosion, oxidation, or other forms of material degradation, which affect the structural integrity and performance of mechanical components. Understanding the kinetics of these reactions helps in predicting how quickly materials will degrade under specific conditions, allowing for the design of protective coatings or treatments to mitigate wear. Additionally, chemical reactions can be involved in lubrication processes, where the kinetics of reactions between lubricants and surfaces can impact friction and wear rates, thereby affecting system reliability and longevity.

Gusmão et al. [31] have applied the modified PINNs as a surrogate approximator for the solution of microkinetic models (MKMs) under the mean-field approximation [32], calling this approach kinetics-informed neural networks. If $c$ represents an array of concentrations or concentration-related state variables like partial pressures, concentrations and coverage fractions, for species that are unbound (like gases) or bound (adsorbed molecules or radicals), at time $t$, then their rates of change, $\dot{c}$, or the MKM, is written as

$$\dot{c}=\mathrm{Mr}\left(c,\theta\right)=\mathrm{M}\left(k\left(\theta\right)\circ f\left(c\right)\right), \tag{8}$$

where $\mathrm{M}\in\mathbb{Z}^{n\times m}$ is the corresponding stoichiometry matrix and $f\left(\cdot\right):\mathbb{R}^n\to\mathbb{R}_+^m$ maps the concentrations $c:=\left\{c\middle|c\in\mathbb{R}_+^n\right\}$ to the concentration-based terms of power-law kinetics,

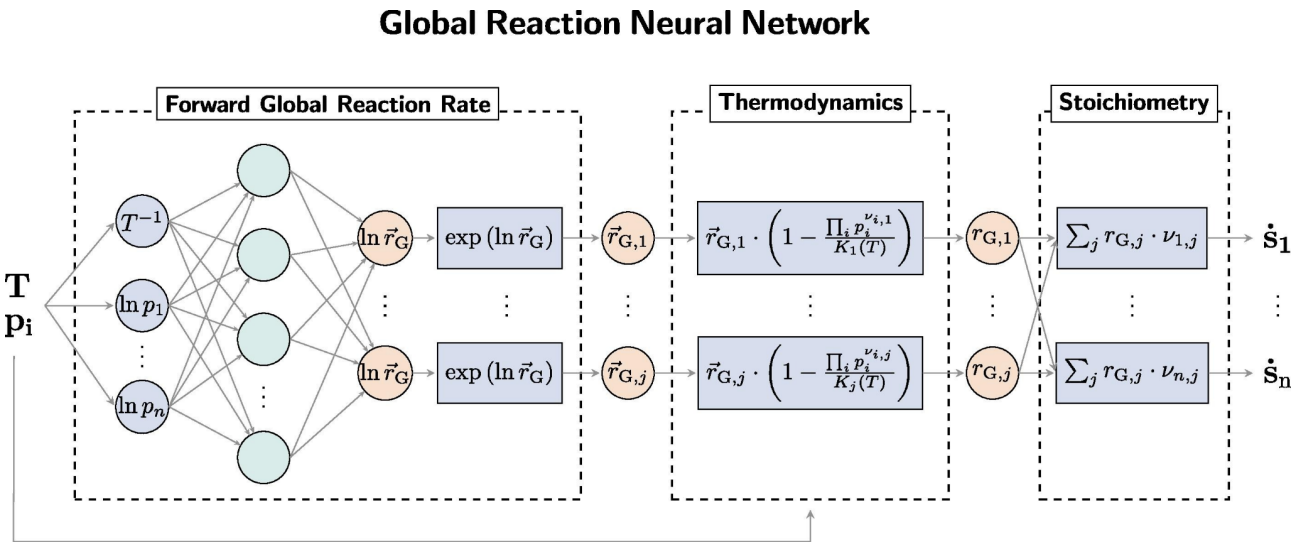


**Fig. 8.** Global reaction neural network architecture with embedded stoichiometry and thermodynamics. The architecture maps the catalyst temperature $T$ and reactant partial pressures $p$ to the steady state gas phase source terms $\dot{s}$. Key features of the architecture are the neural network that outputs the logarithmic forward global rates $\ln(r \to G)$, an exponential mapping to the forward global rates $r \to G$, calculation of thermodynamically consistent global rates $rG$ using the equilibrium constant $K$ and the calculation of stoichiometrically consistent gas species source terms by the stoichiometry $v$. Embedded physical knowledge is highlighted in blue, latent variables of interest are highlighted in red and latent variables of the hidden layers are highlighted in green. Reprinted from Ref. [33], © 2024 T. Kircher, F.A. Döppel, M. Votsmeier. Available under the terms of the CC BY 4.0 license.

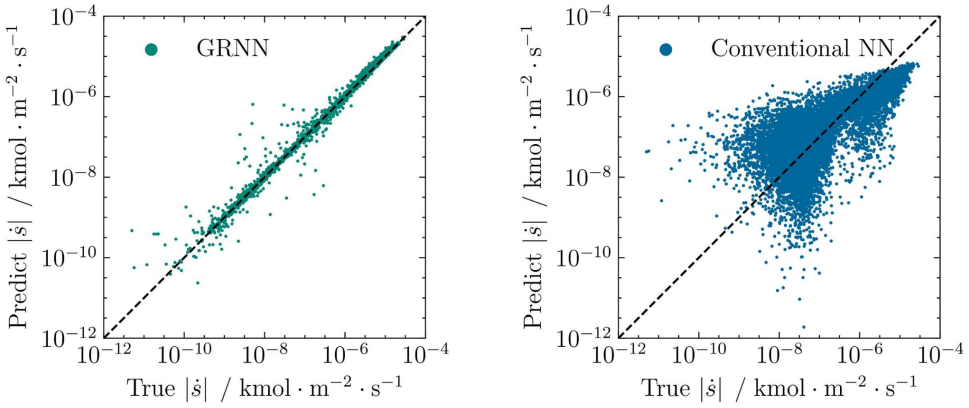


a) GRNN b) Conventional NN

**Fig. 9.** Parity plots of ground truth chemical source terms on the test dataset and source terms predicted by (a) GRNN model and (b) conventional neural network with similar number of model parameters. The GRNN has 1003 parameters using a hidden layer with 100 nodes and the conventional neural network has 1001 parameters using a hidden layer with 83 nodes. The models are trained on data from the same 20 reactor measurements by a fixed step Runge–Kutta fourth order ODE solver. Reprinted from Ref. [33], © 2024 T. Kircher, F.A. Döppel, M. Votsmeier. Available under the terms of the CC BY 4.0 license.

and $k := \left\{k(\theta) \in \mathbb{R}_+^m, \theta \in \mathbb{R}_+\right\}$ is the temperature- and binding-energy-dependent Arrhenius-like rate constant term.

This approach provides an immediate understanding of the extent or depth of dissociation between the observable or measurable states and the underlying intermediates, and hence the complexity of attempting mechanism elucidation. The suitability of neural networks as basis functions for the solution of ODEs is demonstrated by their ability to solve kinetic forward problems.

Furthermore, Kircher et al. [33] have developed an approach embedding stoichiometric and thermodynamic information for learning global reaction kinetics, thus proposing a new global reaction neural network (GRNN) architecture (Fig. 8.).

To enable learning kinetics directly from reactor data, the new neural network is combined with a reactor model and trained using a neural ODE approach. The obtained model could reproduce the molar flow and temperature profiles in 900 further reactor simulations used as test data with a mean error of less than 0.05%. Furthermore, the ground truth source terms were recovered with a mean error of 4.3% (Fig. 9). This approach may still be in the de-

velopment stage, but the ability to study true kinetics opens the door to applying the trained model to different reactor geometries and new applications in tribometry problems.

### 2.6. Wetting

Considering the broader aspect of surface interactions and lubrication, which can involve lipophilic or hydrophobic properties, the wetting characteristics strongly influence the reliability and durability of mechanical systems. In systems where lubricants are used, the interaction between the lubricant and the surface can affect friction and wear. For instance, lipophilic surfaces might interact differently with lubricants, potentially impacting the effectiveness of lubrication and thus the wear rate. Considering a wetting problem, Pan et al. [34] have proposed a network architecture for solving the Young–Laplace (Y–L) equation in the tube domain. Based on the given small amount of data with some noise and in combination with the Y–L equation and Young's equation, the Y–L PINN method can successfully identify the shape of the meniscus, dimensionless Bond number and contact angle θ. Fig. 10 shows the results of the predicted solutions of Y–L PINN for meniscus in the capillary (Fig. 10a). Neither Jurin's law nor the modified Jurin's law can effectively describe the true height of the liquid surface in large-diameter tubes. However, the results obtained using the Y–L PINN method are consistent with the numerical results and the calculations from other works (Fig. 10b). The maximum relative error in the Y–L PINN identification of the meniscus profile with a data quantity of 5 and under 1% noise does not exceed $1.3\times10^{-2}$% (Figs. 10c–e).

Simultaneously, Kiyani et al [35] have taken a different approach based on multiphase many-body dissipative particle dynamics simulations to study the wetting dynamics of highly viscous molten sand droplets. Considering the material to be a liquid mixture of calcium, magnesia, alumina and silicate (CMAS), they have used the PINN framework to identify the parameters of ODEs for the droplets spreading radius behavior (Fig. 11). Considering α to be the main parameter, regulating the dynamics of droplet radius through time $r \sim t^{\alpha}$, sigmoid-type dependence α was taken into consideration

$$\frac{\mathrm{d}\ln r}{\mathrm{d}\ln t} = \alpha\left(t, R_0, \theta_{eq}\right) = \eta\left[\frac{1}{1+\exp\left(\beta\left(\tau-\ln t\right)\right)} - 1\right], \qquad (9)$$

where $r$ is the radius of the wetted area, $t$ is time, $R_0$ is the initial droplet radius, $\theta_{eq}$ is the equilibrium contact angle, unknown parameters η, β and τ were derived with PINN. Subsequently, the closed-form dependency of parameter values found by the PINN on the initial radii and contact angles are given using symbolic regression, and then Bayesian PINNs were employed to assess and quantify the uncertainty associated with the discovered parameters. The close alignment between the discovered parameters in both models demonstrates the robustness and reliability of these models. It highlights their ability to capture effectively the underlying dynamics and characteristics of the spreading behaviour of CMAS, leading to accurate parameter estimation. The relationships uncovered and methods developed in this study have broader applications in understanding the spreading dynamics of droplets in general. By leveraging the insights gained from this research, one can investigate and understand the behaviour of droplets in diverse contexts, furthering our understanding of droplet spreading phenomena. Potentially, this knowledge can be used in developing strategies for effective droplet management and optimizing processes involving droplets in a wide range of practical applications, including those related to the tribometry problems.

### 2.7. Phase transitions

PINNs have emerged as a powerful tool for modeling complex material behaviors and structural transformations. They have been successfully applied to microstructure-sensitive modeling and inverse design problems in materials science, predicting texture evolution and calibrating crystal plasticity parameters [36–38]. PINNs have shown the ability to effectively solve the specific PDEs, dealing with heat propagation in a liquid-solid phase change system (Stefan problem) [39]. The primary benefit lies in PINNs' capacity to simulate dynamic structural evolution, such as shear-induced layering and grain size reduction, which govern wear resistance and mechanical stability. By incorporating dislocation reaction kinetics and stress-dependent phase transitions, these models unravel mechanisms like tribologically driven amorphization or subsurface recrystallization observed in alloys under cyclic loading. Their mesh-free framework efficiently handles 3D contact geometries and time-varying loads, enabling predictive insights into how localized stress fields initiate dislocation patterning or interfacial phase transformations [40]. This approach supports tailored material design by linking microstructural outcomes to loading parameters without relying on idealized boundary conditions. Wight and Zhao [41] have shown that PINN inaccuracies while solving the Allen-Cahn and the Cahn-Hilliard equations can be avoided by several approximating strategies. Improved PINNs are shown to be used to solve the phase field equations of increased complexity. Ning et al. [42] have established an improved PINN model based on a peridynamic approach (PD-INN) to characterize displacements in elastic plates. The four considered cases showed that the proposed PD-INN can generally predict the displacement distribution in homo-

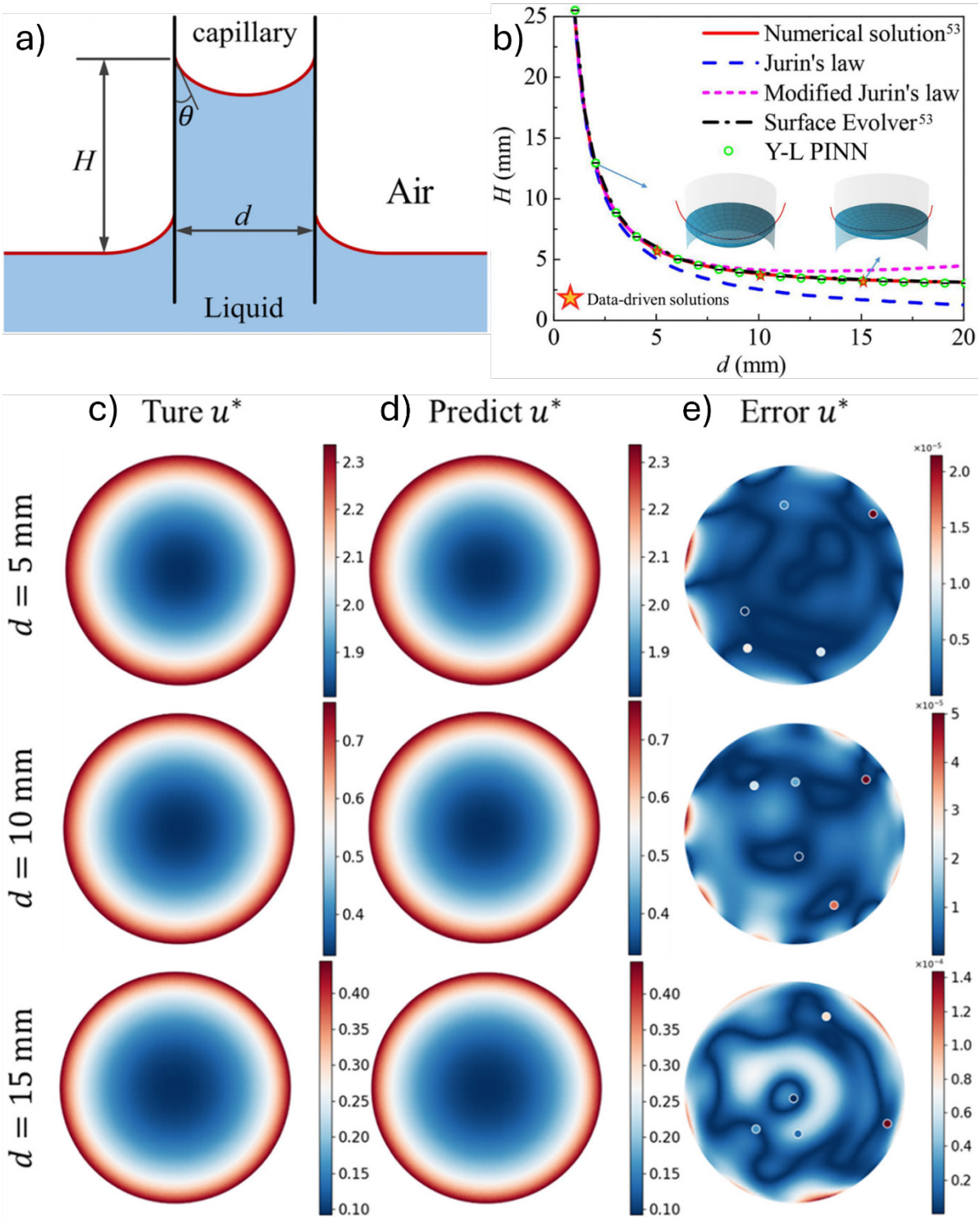


**Fig. 10.** (a) Schematic of the capillary rise. A liquid column of height $H$ in a capillary with diameter $d$ and contact angle θ. (b) The variation pattern of the meniscus height $H$ with the tube diameter $d$. The stars represent the Y–L PINN models obtained from training with tube diameters of 5, 10, and 15 mm. (c–e) Under 1% noise and a data quantity of 5, the comparison between the predicted solutions of Y–L PINN and the true meniscus profile $u$ is presented for different tube diameters. (c) The true solutions of the Young–Laplace equation for the three tube diameters. (d) The computed results of Y–L PINN for the corresponding tube diameters. (e) The relative error of Y–L PINN. The positions of the data points are represented by dots, while the color indicates the height values. Adapted from Ref. [34].

geneous and heterogeneous plates. However, challenges associated with network training and prediction accuracy remain. That main challenge is the programming difficulty of the PD-INN, limiting its practicability. More importantly, the convergence speed of the network and the number of sampling points is said to be further increased to improve the characterization accuracy in complex heterogeneous plates. The PD-INN can theoretically approximate

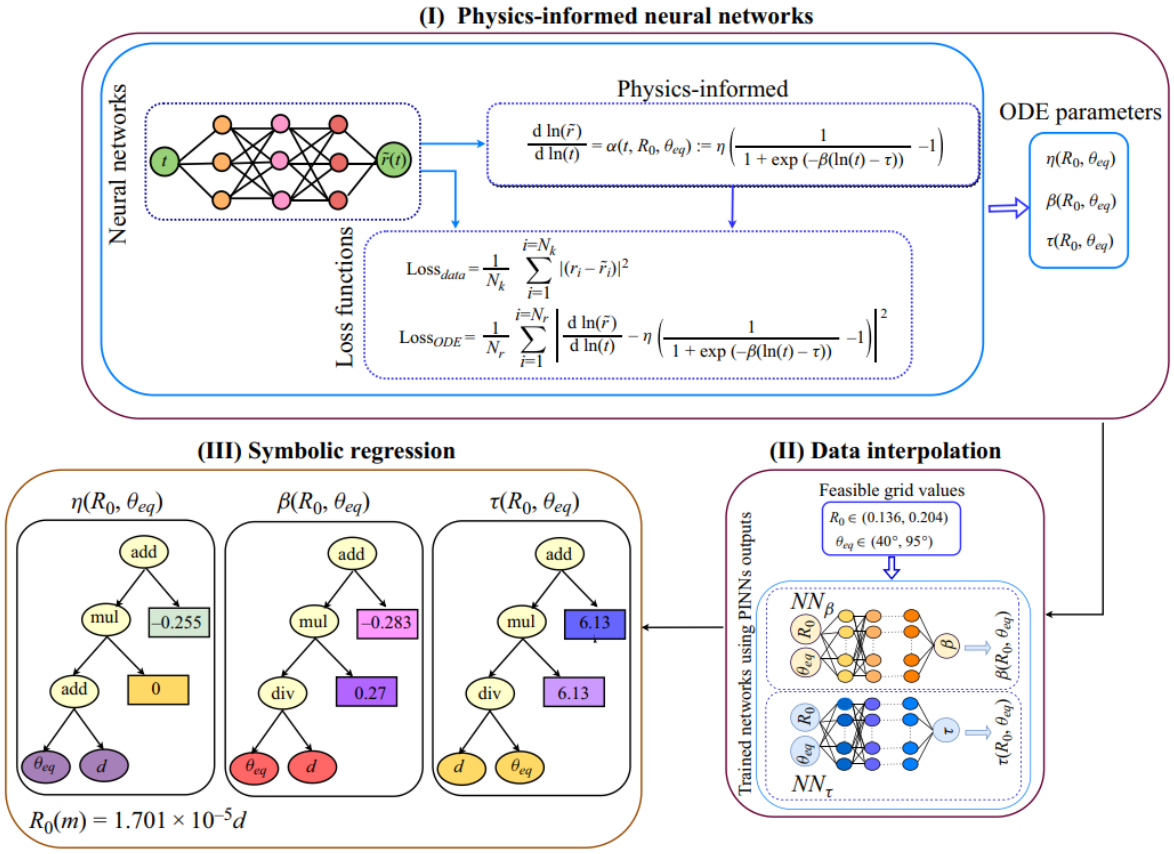


**Fig. 11.** The process of utilizing PINNs to extract three unknown parameters of the ODE, using three-dimensional multiphase many-body dissipative particle dynamics simulation data. First, a neural network is trained using simulation data, where the input is time $t$ and the output is spreading radii $\tilde{r}(t)$. This neural network comprises four layers with three neurons, and is trained for 12 000 epochs. Subsequently, the predicted $\tilde{r}(t)$ is used to satisfy Eq. (9) in the physics-informed part. The loss function for this process consists of two parts: data matching and residual. By optimizing the loss function, the values of $\eta(R_0,\theta_{eq})$, $\beta(R_0,\theta_{eq})$ and $\tau(R_0,\theta_{eq})$ are determined for each set of $R_0$ and $\theta_{eq}$. After predicting the unknown parameters using PINNs, two additional neural networks, denoted as $NN_\beta$ and $NN_\tau$, are trained using these parameters to generate values for the unknown parameters at points where data are not available. The outputs of these networks, together with the outputs of the PINNs, are then fed through a symbolic regression model to discover a mathematical expression for the discovered parameter. Reprinted from Ref. [35], © 2024 E. Kiyani et al. Available under the terms and conditions of the CC BY-NC-SA 4.0 license.

a crack propagation problem (see the next Section) with numerous time-consuming iterations, requiring hundreds of thousands of epochs for network convergence.

### 2.8. Cracking and fretting

PINNs have shown ability to model complex phenomena like cracking and fretting during contact load. PINNs have been applied to predict fretting fatigue lifetime by combining experimental data with physics equations [43]. They have also been used to simulate crack initiation and propagation in quasi-brittle plates by minimizing peridynamic potential energy [42]. For fatigue life prediction, PINNs have demonstrated accuracy with small datasets by incorporating physical models into the network architecture [44]. This ability was proven to be applicable to model and predict crack lengths in elements of critical infrastructure, for example, in gas turbine components, specifically in first-stage injectors [45]. Presented model based on recurrent neural network (Fig. 12) uses real data from turbines (such as temperatures and pressures) and is based on the Paris' law crack growth equation, which relates stress in a material to how quickly a crack lengthens. Also, in corrosion-fatigue prognosis, a hybrid approach combining physics-informed and data-driven layers has been developed to model crack growth and corrosion effects in aircraft wing panels [46]. These and following studies highlight the versatility of PINNs in addressing various aspects of material degradation and failure, offering improved accuracy and physical consistency compared to traditional methods.

Goswami et al. [47] proposed in 2019 a new approach to solving fracture mechanics problems using PINNs focused on phase-field modeling of brittle fracture. While

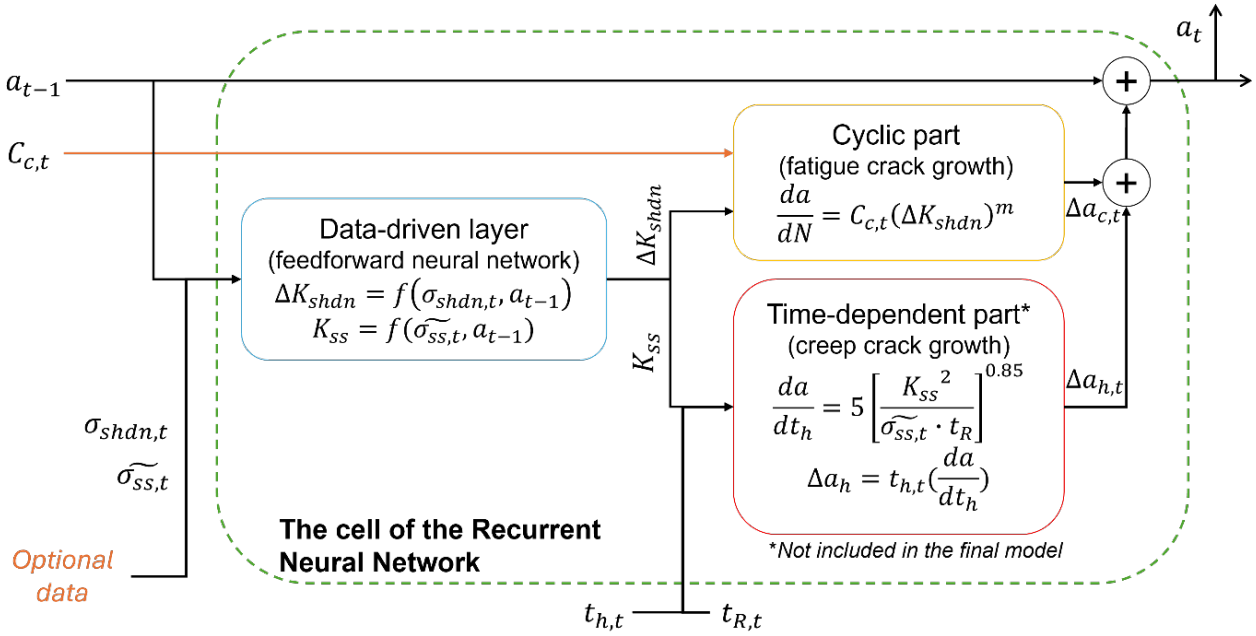


**Fig. 12.** The custom cell of the physics-informed recurrent neural network. This figure is a sketch of Fig. 7 from Ref. [45]; all major designations are saved.

most of the PINN algorithms available in the literature minimize the residual of the governing PDE, the proposed approach takes a different path by minimizing the variational energy of the system. This reduces the order of derivatives required for calculations and increases the stability and speed of training the neural network. For numerical integration of the variational energy, the Gauss–Legendre quadrature method is used, which, in combination with non-uniform rational B-splines (NURBS), allows for an accurate description of the crack geometry and local refinement of the mesh along the fracture path. A transfer learning technique is also implemented, in which the neural network is partially trained for each new load step: only the parameters of the last layer are updated, while the rest remain fixed, which dramatically reduces the computational costs of crack growth calculations.

Recently, Lian et al. [48] showed the so-called phase field fracture model, which describes the propagation of cracks not through explicit tracking of discontinuities, but using a continuous phase field, which simplifies numerical calculations of complex crack geometry. The authors proposed to improve the accuracy of the model by implementing length-scale decoupling degradation functions, which made it possible to reduce the density of the resolution grid of diffuse fracture zones and increase the efficiency of modeling.

Yucesan et al. [49] presented a model combining physics and machine learning to predict the fatigue wear of onshore wind turbine bearings using PINNs. Traditional standard-based approaches do not take into account complex factors such as lubricant degradation, which limits their accuracy. The authors propose a recurrent neural network architecture, where physical equations model the accumulation of fatigue damage (Palmgren-Miner method) and lubricant condition data are processed by a multilayer perceptron. The physical part of the model includes the calculation of bearing life taking into account dynamic loads, temperature, and lubricant contamination. Lubricant data affecting viscosity and contamination are modeled by data obtained by simulating real contamination in the laboratory.

Shukla et al. [50] presented a method for using PINN for non-destructive assessment of surface cracks in metal plates using ultrasonic surface acoustic waves. Cracks are identified by analyzing the local change in the speed of sound caused by scattering and attenuation of waves in the defect area. The results demonstrate that the presence of a crack leads to a decrease in the effective velocity in the zone affected by the crack. This decrease in velocity is due to the backscattering of waves from the crack, which ultimately leads to a loss of wave energy. The PINN model integrates the acoustic wave equation into the loss function, which allows combining physical hypotheses with experimental data.

Finally, Wang et al. [43] used data from 27 laboratory tests on aluminum alloy, in which they created models of the contact of parts, taking into account friction and loads. PINN predicted wear more accurately than a conventional neural network. An important role was played by the choice of parameters that determine “how much physics” was taken into account in the neural network. In the proposed approach, the stress distribution is calculated

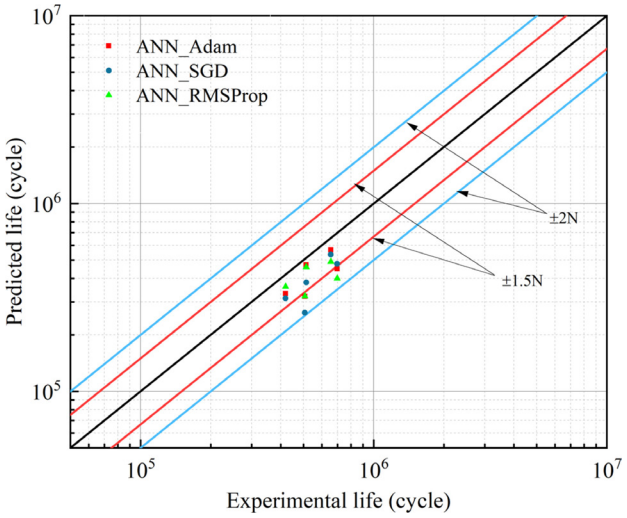


**Fig. 13.** Prediction results from ANN models versus experimental results. Adam is adaptive moment estimation, SGD is stochastic gradient descent algorithm, RMSProp is root mean square propagation. Among the three ANN models, the one using the Adam algorithm produced the best results, with data points closely aligning with the black line. Reprinted from Ref. [43], 

by FEM using the critical plane method, forming a database for training an artificial neural network (ANN). Then, physics laws are integrated into the data-assisted PINN architecture, including the Findley parameter relationship with cyclic loads, which allows the model to combine experimental data with fundamental equations of mechanics, increasing the accuracy of predictions (Fig. 13).

## 3. OUTLOOK AND CONCLUSIONS

There are three aspects in the problem of data availability and validity in realistic tribological systems containing materials with surface roughness that have not yet been sufficiently explored in the domain of PINNs research: surface roughness data, local tribometric data and contact mechanics simulation data.

### 3.1. Surface roughness

In the numerous multiphysics phenomena shown in the Fig. 1, surface roughness plays one of the most important roles for tribological properties of contact system.

Computational tribology models commonly rely on the surface roughness data described as surface roughness power spectrum. Power spectrum density (PSD) is a common way to describe surface roughness as reviewed in Refs. [51] and [52]. However, PSD does not contain full information on surface topography, namely phase components of the spectrum are lost. Thus, different surfaces can have same PSD.

There is a debate on the experimental methods most applicable for obtaining surface topography data. In Ref. [53], it is demonstrated that surface height data obtained using optical methods can be often inaccurate and should be avoided in calculating surface roughness power spectra, while engineering stylus instruments and atomic force microscopy should be generally preferred. For surfaces with isotropic roughness, the tribologically relevant information about the roughness is contained in a line scan and can be converted to 2D power spectrum.

Silicone elastomer can be used to obtain replica of surfaces and measuring PSD which are difficult to evaluate directly, including surfaces with very high roughness [54].

Surface roughness can be created in numerical simulations by randomization algorithms [55–58].

### 3.2. Analytical (local) tribometry

Many traditional experimental tribology techniques commonly are measurements of “global” quantities. They represent integral quantities in the tribological interface, such as friction force represents the integral of interfacial shear stress over contact area. However, taking into account various local quantities is crucial for accurate tribological modeling. Those local quantities can include real area of contact, local deformation, temperature distribution.

Analytical tribometry can be defined as a set of experimental instruments that allow collect local data beyond the traditional friction force / applied force / displacement / velocity variables. In recent years, measurement of local quantities has become more accessible due to new available instruments and techniques. One of the most important types of local data in analytical tribometry includes optical observation of the contact patches for contact loaded both in normal and shear modes. This can, e.g., include optical imaging further processed with digital image correlation method [59].

Experimental optical observation of contact area with surface roughness for elastomers/glass had been demonstrated in the works [60,61]. Optical contact observation for rough surfaces using rigidochromic molecules was recently also demonstrated in Ref. [62].

Another examples of analytical tribometry include infrared thermography method that can be used to detect frictional heating [63], spectrometer-equipped instrument for studying tribochemical processes [64].

Imagining techniques allow obtaining data that would be difficult to get by other means, but they have limitations, because the contact materials must be transparent. Alternative approach to collecting local data, taken by academic tribologists, is considering micro- and nanoscale single asperity systems. Single asperity tribological sys-

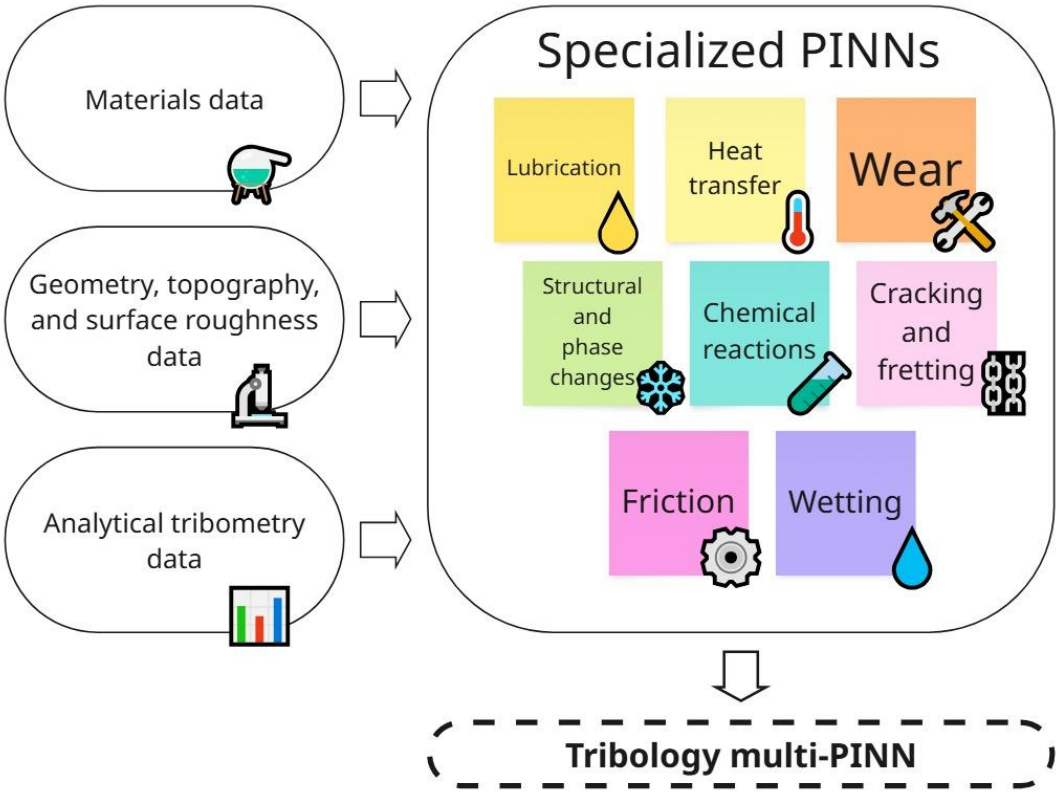


**Fig. 14.** Diagram of integration of specialized tribology-related PINNs into a synthesized multiphysics-aware tribology PINN.

tems can be useful to abstract the effects of surface roughness and long-range mechanical coupling.

### 3.3. Contact mechanics numerical simulations with rough surfaces

State of the real surfaces in contact is difficult to define due to the surface roughness and contaminations that are heavily affecting contact phenomena. Once theoretically defined such a surface contains incredible number of degrees of freedom. There are numerous computational methods allowing treatment of tribological systems with many degrees of freedom [4], some of them are specialized for tribological problems.

The "classical" approaches to contact mechanics neglect non-local elastic deformation in the body with surface roughness [65,66]. On the other hand, FEM allows to solve the continuum elasticity problem accurately, but can require large computational resources for systems with surface roughness. Boundary element methods [56] and Green's function molecular dynamics (GFMD) reduce computational requirements by modeling only contacting surfaces, thus, present in this regard a computationally efficient alternative. In particular, GFMD [67–69] enables efficient scaling through parallelization as reviewed in Ref. [70]. It must be noted that GFMD can be both applied on the level of discrete atoms as well as in the continuum mechanics limit [71,72].

The tribological applications are fundamentally dependent on a variety of multiphysics phenomena (Fig. 1) that need to be taken into account in creating PINNs. Improving accuracy of PINNs predictions would require input that includes materials data, topography and surface roughness, and miscellaneous data of analytical tribometry. Creating an integrated PINN ("multi-PINN") that is capable of synthesizing the individual tribology-related phenomena presents a practically important and challenging problem (Fig. 14) that is yet at the dawn of academic research.

## ACKNOWLEDGEMENTS

The research was supported by ITMO University Research Projects in AI Initiative (RPAII) (project #640114).

## REFERENCES

[1] D. Dowson, *History of Tribology, 2nd Edition*, Professional Engineering Publishing, London, 1998
[2] B.N.J. Persson, *Sliding Friction*, in: P. Avouris, B. Bhushan, D. Bimberg, C.-Z. Ning, K. von Klitzing, R. Wiesendanger (Series Eds.), Book Series: NanoScience and Technology, Springer Berlin, Heidelberg, 2000.
[3] A.I. Vakis et al., Modeling and Simulation in Tribology across Scales: An Overview, *Tribology International*, 2018, vol. 125, pp. 169–199.
[4] M.H. Müser et al., Meeting the Contact-Mechanics Challenge, *Tribology Letters*, 2017, vol. 65 no. 4, art. no. 118.

[5] E. Gnecco, E. Meyer (Eds.), *Fundamentals of Friction and Wear on the Nanoscale, 2nd Ed.*, in: P. Avouris, B. Bhushan, D. Bimberg, C.-Z. Ning, K. von Klitzing, R. Wiesendanger (Series Eds.), Book Series: NanoScience and Technology, Springer Cham, 2015.
[6] E. Gnecco, E. Meyer, *Elements of Friction Theory and Nanotribology*, Cambridge University Press, 2015.
[7] M. Marian, S. Tremmel, Physics-Informed Machine Learning—An Emerging Trend in Tribology, *Lubricants*, 2023, vol. 11, no. 11, art. no. 463.
[8] R. Shah, R. Jaramillo, G. Thomas, T. Rayhan, N. Hossain, M. Kchaou, F.J. Profito, A. Rosenkranz, Artificial Intelligence and Machine Learning in Tribology: Selected Case Studies and Overall Potential, *Advanced Engineering Materials*, 2025, art. no. 2401944.
[9] M. Marian, S. Tremmel, Current Trends and Applications of Machine Learning in Tribology—A Review, *Lubricants*, 2021, vol. 9, no. 9, art. no. 86.
[10] L Samylingam et al., Enhancing Lubrication Efficiency and Wear Resistance in Mechanical Systems through the Application of Nanofluids: A Comprehensive Review, *Journal of Advanced Research in Micro and Nano Engineering*, 2024, vol. 16, no. 1, pp. 1–18.
[11] F. Brumand-Poor, F. Barlog, N. Plückhahn, M. Thebelt, N. Bauer, K. Schmitz, Physics-Informed Neural Networks for the Reynolds Equation with Transient Cavitation Modeling, Lubricants, 2024, vol. 12, no. 11, art. no. 365.
[12] Y. Zhao, P.P.L. Wong, A Hybrid Data-Driven Approach for the Analysis of Hydrodynamic Lubrication, *Proceedings of the Institution of Mechanical Engineers, Part J: Journal of Engineering Tribology*, 2024, vol. 238, no. 3, pp. 320–331.
[13] M. Rom, Physics-Informed Neural Networks for the Reynolds Equation with Cavitation Modeling, *Tribology International*, 2023, vol. 179, art. no. 108141.
[14] A. Almqvist, Fundamentals of Physics-Informed Neural Networks Applied to Solve the Reynolds Boundary Value Problem, *Lubricants*, 2021, vol. 9, no. 8, art. no. 82.
[15] G. Zhou, M. Zhan, D. Huang, X. Lyu, K. Yan, Enhanced PINNs with Augmented Lagrangian Method and Transfer Learning for Hydrodynamic Lubrication Analysis, *Industrial Lubrication and Tribology*, 2024, vol. 76, no. 10, pp. 1246–1255.
[16] G. Wszelaczyński, D. Capanidis, M. Paszkowski, T. Leśniewski, *Operating Problems of Lubrication of Friction Nodes in Mining Machines Working in an Aggressive Environment*, in: J. Stryczek, U. Warzyńska (Eds.), Advances in Hydraulic and Pneumatic Drives and Control 2020, Book Series: Lecture Notes in Mechanical Engineering, Springer, Cham, 2021, pp. 228–238.
[17] P. Olejnik, S. Ayankoso, Friction Modelling and the Use of a Physics-Informed Neural Network for Estimating Frictional Torque Characteristics, *Meccanica*, 2023, vol. 58, pp. 1885–1908.
[18] Y. Xia, Y. Meng, Physics-Informed Neural Network (PINN) for Solving Frictional Contact Temperature and Inversely Evaluating Relevant Input Parameters, *Lubricants*, 2024, vol. 12, no. 2, art. no. 62.
[19] J. Jakubowski, P. Stanisz, S. Bobek, G.J. Nalepa, Roll Wear Prediction in Strip Cold Rolling with Physics-Informed Autoencoder and Counterfactual Explanations, in: *2022 IEEE 9th International Conference on Data Science and Advanced Analytics (DSAA)*, IEEE, Shenzhen, China, 2022, pp 1–10.
[20] K. Zhu, H. Guo, S. Li, X. Lin, Physics-Informed Deep Learning for Tool Wear Monitoring, *IEEE Transactions on Industrial Informatics*, 2024, vol. 20, no. 1, pp. 524–533.
[21] A.L.B. Dos Santos, M.A.V. Duarte, A.M. Abrão, A.R. Machado, An Optimisation Procedure to Determine the Coefficients of the Extended Taylor's Equation in Machining, *International Journal of Machine Tools and Manufacture*, 1999, vol. 39, no. 1, pp. 17–31.
[22] V. Prasanth, R. Sharma, M. Ramachandran, S. Chinnasamy, Evaluation of Automotive Brake Disc Material Selection Using Weighted Sum Method (WSM), *REST Journal on Advances in Mechanical Engineering*, 2024, vol. 3, no. 3, pp. 9–18.
[23] R. Miyazawa, H. Mori, A. Horibe, Thermal and Mechanical Analysis of Embedded Liquid Cooling with Microchannel and Pin-Fin Structures, in: *2024 23rd IEEE Intersociety Conference on Thermal and Thermomechanical Phenomena in Electronic Systems (ITherm)*, IEEE, Aurora, CO, USA, 2024, pp 1–8.
[24] Q. Zhang, X. Guo, X. Chen, C. Xu, J. Liu, PINN-FFHT: A Physics-Informed Neural Network for Solving Fluid Flow and Heat Transfer Problems without Simulation Data, *International Journal of Modern Physics C*, 2022, vol. 33, no. 12, art. no. 2250166.
[25] S. Cai, Z. Wang, S. Wang, P. Perdikaris, G.E. Karniadakis, Physics-Informed Neural Networks for Heat Transfer Problems, *Journal of Heat Transfer*, 2021, vol. 143, no. 6, art. no. 060801.
[26] H. He, J. Pathak, An Unsupervised Learning Approach to Solving Heat Equations on Chip Based on Auto Encoder and Image Gradient, *arXiv*, 2020, art. no. 2007.09684.
[27] R. Laubscher, Simulation of Multi-Species Flow and Heat Transfer Using Physics-Informed Neural Networks, *Physics of Fluids*, 2021, vol. 33, no. 8, art. no. 087101.
[28] M.M. Billah, A.I. Khan, J. Liu, P. Dutta, Physics-Informed Deep Neural Network for Inverse Heat Transfer Problems in Materials, *Materials Today Communications*, 2023, vol. 35, art. no. 106336.
[29] N. Zobeiry, K.D. Humfeld, A Physics-Informed Machine Learning Approach for Solving Heat Transfer Equation in Advanced Manufacturing and Engineering Applications, *Engineering Applications of Artificial Intelligence*, 2021, vol. 101, art. no. 104232.
[30] L.-T. Zhu, X.-Z. Chen, B. Ouyang, W.-C. Yan, H. Lei, Z. Chen, Z.-H. Luo, Review of Machine Learning for Hydrodynamics, Transport, and Reactions in Multiphase Flows and Reactors, *Industrial & Engineering Chemistry Research*, 2022, vol. 61, no. 28, pp. 9901–9949.
[31] G.S. Gusmão, A.P. Retnanto, S.C.D. Cunha, A.J. Medford, Kinetics-Informed Neural Networks, *Catalysis Today*, 2023, vol. 417, art. no. 113701.
[32] N. Cheimarios, Mean Field Approximation of a Surface-Reaction Growth Model with Dissociation, *Physics Letters A*, 2024, vol. 524, art. no. 129828.
[33] T. Kircher, F.A. Döppel, M. Votsmeier, Global Reaction Neural Networks with Embedded Stoichiometry and Thermodynamics for Learning Kinetics from Reactor Data, *Chemical Engineering Journal*, 2024, vol. 485, art. no. 149863.
[34] C. Pan, S. Feng, S. Tao, H. Zhang, Y. Zheng, H. Ye, Physics-Informed Neural Network for Solving Young–Laplace Equation and Identifying Parameters, *Physics of Fluids*, 2024, vol. 36, no. 2, art. no. 022116.
[35] E. Kiyani, M. Kooshkbaghi, K. Shukla, R.B. Koneru, Z. Li, L. Bravo, A. Ghoshal, G.E. Karniadakis, M. Kart-

tunen, Characterization of Partial Wetting by CMAS Droplets Using Multiphase Many-Body Dissipative Particle Dynamics and Data-Driven Discovery Based on PINNs, *Journal of Fluid Mechanics*, 2024, vol. 985, art. no. A7.

[36] J. Rogal, E. Schneider, M.E. Tuckerman, Neural-Network-Based Path Collective Variables for Enhanced Sampling of Phase Transformations, *Physical Review Letters*, 2019, vol. 123, no. 24, art. no. 245701.

[37] A. Henkes, H. Wessels, R. Mahnken, Physics Informed Neural Networks for Continuum Micromechanics, *Computer Methods in Applied Mechanics and Engineering*, 2022, vol. 393, art. no. 114790.

[38] M. Hasan, Z. Ender Eger, A. Senthilnathan, P. Acar, Microstructure-Sensitive Deformation Modeling and Materials Design with Physics-Informed Neural Networks, *AIAA Journal*, 2024, vol. 62, no. 5, pp. 1864–1874.

[39] B.-E. Madir, F. Luddens, C. Lothodé, I. Danaila, Physics Informed Neural Networks for Heat Conduction with Phase Change, *arXiv*, 2024, art. no. 2410.14216.

[40] S. Lee, J. Popovics, Applications of Physics-Informed Neural Networks for Property Characterization of Complex Materials, *RILEM Technical Letters*, 2023, vol. 7, pp. 178–188.

[41] C.L. Wight, J. Zhao, Solving Allen-Cahn and Cahn-Hilliard Equations Using the Adaptive Physics Informed Neural Networks, *Communications in Computational Physics*, 2021, vol. 29, no. 3, pp. 930–954.

[42] L. Ning, Z. Cai, H. Dong, Y. Liu, W. Wang, A Peridynamic-Informed Neural Network for Continuum Elastic Displacement Characterization, *Computer Methods in Applied Mechanics and Engineering*, 2023, vol. 407, art. no. 115909.

[43] C. Wang, Q. Xiao, Z. Zhou, Y. Yang, G. Kosec, L. Wang, M. Abdel Wahab, A Data-assisted Physics-informed Neural Network (DA-PINN) for Fretting Fatigue Lifetime Prediction, *International Journal of Mechanical System Dynamics*, 2024, vol. 4, no. 3, pp. 361–373.

[44] D. Chen, Y. Li, K. Liu, Y. Li, A Physics-Informed Neural Network Approach to Fatigue Life Prediction Using Small Quantity of Samples, *International Journal of Fatigue*, 2023, vol. 166, art. no. 107270.

[45] M. Badora, P. Bartosik, A. Graziano, T. Szolc, Using Physics-Informed Neural Networks with Small Datasets to Predict the Length of Gas Turbine Nozzle Cracks, *Advanced Engineering Informatics*, 2023, vol. 58, art. no. 102232.

[46] A. Dourado, F.A.C. Viana, Physics-Informed Neural Networks for Corrosion-Fatigue Prognosis, *Proceedings of the Annual Conference of the PHM Society*, 2019, vol. 11, no. 1.

[47] S. Goswami, C. Anitescu, S. Chakraborty, T. Rabczuk, Transfer Learning Enhanced Physics Informed Neural Network for Phase-Field Modeling of Fracture, *Theoretical and Applied Fracture Mechanics*, 2020, vol. 106, art. no. 102447.

[48] H. Lian, P. Zhao, M. Zhang, P. Wang, Y. Li, Physics Informed Neural Networks for Phase Field Fracture Modeling Enhanced by Length-Scale Decoupling Degradation Functions, *Frontiers in Physics*, 2023, vol. 11, art. no. 1152811.

[49] Y.A. Yucesan, F.A.C. Viana, A Physics-Informed Neural Network for Wind Turbine Main Bearing Fatigue, *International Journal of Prognostics and Health Management*, 2023, vol. 11, no. 1.

[50] K. Shukla, P.C. Di Leoni, J. Blackshire, D. Sparkman, G.E. Karniadakis, Physics-Informed Neural Network for Ultrasound Nondestructive Quantification of Surface Breaking Cracks, *Journal of Nondestructive Evaluation*, 2020, vol. 39, no. 3, art. no. 61.

[51] T.D.B. Jacobs, T. Junge, L. Pastewka, Quantitative Characterization of Surface Topography Using Spectral Analysis, *Surface Topography: Metrology and Properties*, 2017, vol. 5, no. 1, art. no. 013001.

[52] F.M. Borodich, A. Pepelyshev, O. Savencu, Statistical Approaches to Description of Rough Engineering Surfaces at Nano and Microscales, *Tribology International*, 2016, vol. 103, pp. 197–207.

[53] N. Rodriguez, L. Gontard, C. Ma, R. Xu, B.N.J. Persson, On How to Determine Surface Roughness Power Spectra, *Tribology Letters*, 2025, vol. 73, no. 1, art. no. 18.

[54] J.S. Persson, A. Tiwari, E. Valbahs, T.V. Tolpekina, B.N.J. Persson, On the Use of Silicon Rubber Replica for Surface Topography Studies, *Tribology Letters*, 2018, vol. 66, no. 4, art. no. 140.

[55] V.A. Yastrebov, G. Anciaux, J.-F. Molinari, The Role of the Roughness Spectral Breadth in Elastic Contact of Rough Surfaces, *Journal of the Mechanics and Physics of Solids*, 2017, vol. 107, pp. 469–493.

[56] C. Putignano, L. Afferrante, G. Carbone, G. Demelio, A New Efficient Numerical Method for Contact Mechanics of Rough Surfaces, *International Journal of Solids and Structures*, 2012, vol. 49, no. 2, pp. 338–343.

[57] Y.Z. Hu, K. Tonder, Simulation of 3-D Random Rough Surface by 2-D Digital Filter and Fourier Analysis, *International Journal of Machine Tools and Manufacture*, 1992, vol. 32, no. 1–2, pp. 83–90.

[58] P. Meakin, *Fractals, Scaling and Growth Far from Equilibrium*, Cambridge Nonlinear Science Series, Cambridge University Press, Cambridge, 1998.

[59] F. Hild, S. Roux, Digital Image Correlation: From Displacement Measurement to Identification of Elastic Properties – a Review, *Strain*, 2006, vol. 42, no. 2, pp. 69–80.

[60] L. Dorogin, A. Tiwari, C. Rotella, P. Mangiagalli, B.N.J. Persson, Role of Preload in Adhesion of Rough Surfaces, *Physical Review Letters*, 2017, vol. 118, no. 23, art. no. 238001.

[61] L. Dorogin, A. Tiwari, C. Rotella, P. Mangiagalli, B.N.J. Persson, Adhesion between Rubber and Glass in Dry and Lubricated Condition, *The Journal of Chemical Physics*, 2018, vol. 148, no. 23, art. no. 234702.

[62] B. Weber, T. Suhina, T. Junge, L. Pastewka, A.M. Brouwer, D. Bonn, Molecular Probes Reveal Deviations from Amontons' Law in Multi-Asperity Frictional Contacts, *Nature Communications*, 2018, vol. 9, no. 1, art. no. 888.

[63] R. Usamentiaga, P. Venegas, J. Guerediaga, L. Vega, J. Molleda, F. Bulnes, Infrared Thermography for Temperature Measurement and Non-Destructive Testing, *Sensors*, 2014, vol. 14, no. 7, pp. 12305–12348.

[64] F. Mangolini, A. Rossi, N.D. Spencer, In Situ Attenuated Total Reflection (ATR/FT-IR) Tribometry: A Powerful Tool for Investigating Tribochemistry at the Lubricant–Substrate Interface, *Tribology Letters*, 2012, vol. 45, no. 1, pp. 207–218.

[65] A.W. Bush, R.D. Gibson, T.R. Thomas, The Elastic Contact of a Rough Surface, *Wear*, 1975, vol. 35, no. 1, pp. 87–111.

[66] J.A. Greenwood, J.B.P. Williamson, Contact of Nominally Flat Surfaces, *Proceedings of the Royal Society A*, 1966, vol. 295, no. 1442, pp. 300–319.

[67] C. Campañá, M.H. Müser, Practical Green's Function Approach to the Simulation of Elastic Semi-Infinite Solids, *Physical Review B*, 2006, vol. 74, no. 7, art. no. 075420.
[68] L.T. Kong, G. Bartels, C. Campañá, C. Denniston, M.H. Müser, Implementation of Green's Function Molecular Dynamics: An Extension to LAMMPS, *Computer Physics Communications*, 2009, vol. 180, no. 6, pp. 1004–1010.
[69] N. Prodanov, W.B. Dapp, M.H. Müser, On the Contact Area and Mean Gap of Rough, Elastic Contacts: Dimensional Analysis, Numerical Corrections, and Reference Data, *Tribology Letters*, 2014, vol. 53, no. 2, pp. 433–448.
[70] I. Solovyev, V. Petrenko, Y. Murugesan, L. Dorogin, Recent Progress in Contact Mechanics Methods for Solids with Surface Roughness Using Green's Function Molecular Dynamics, *Reviews on Advanced Materials and Technologies*, 2022, vol. 4, no. 1, pp. 1–8.
[71] S.P. Venugopalan, M.H. Müser, L. Nicola, Green's Function Molecular Dynamics Meets Discrete Dislocation Plasticity, *Modelling and Simulation in Materials Science and Engineering*, 2017, vol. 25, no. 6, art. no. 065018.
[72] S.P. Venugopalan, L. Nicola, M.H. Müser, Green's Function Molecular Dynamics: Including Finite Heights, Shear, and Body Fields, *Modelling and Simulation in Materials Science and Engineering*, 2017, vol. 25, no. 3, art. no. 034001.

УДК 539.3

# Развитие и перспективы физически информированных нейронных сетей для трибологических применений с мультифизической интеграцией

**А.Ю. Кохановский [1], Л.М. Дорогин [2,3], К.А. Егорова [4], Е.В. Антонов [2], Д.А. Синев [4]**

[1] Физический факультет, Университет ИТМО, Кронверкский пр., 49, лит. А, Санкт-Петербург, 197101, Россия
[2] Институт перспективных систем передачи данных, Университет ИТМО, Кронверкский пр., 49, лит. А, Санкт-Петербург, 197101, Россия
[3] Department of Molecules and Materials, University of Twente, Enschede, Netherlands
[4] Институт лазерных технологий, Университет ИТМО, Кронверкский пр., 49, лит. А, Санкт-Петербург, 197101, Россия

Аннотация. Представлен краткий обзор последних достижений в области нейронных сетей, основанных на физике (PINN), для приложений, связанных с трибологией. Трибологические приложения рассматриваются как фундаментально зависящие от множества мультифизических явлений, которые необходимо учитывать при создании PINN. Мультифизические входные данные для PINNs могут включать данные о материалах, топографии и шероховатости поверхности, а также данные аналитической трибометрии, которые используются для анализа трения, смазки, износа, смачивания, теплопередачи, структурных и фазовых переходов, химических реакций, растрескивания и фреттинга. Создание мульти-PINN, которые соединяют отдельные трибологические явления, представляет собой практически важную и сложную проблему, которую еще предстоит решить.

*Ключевые слова*: трибология; трение; нейронные сети; мультифизика; машинное обучение